Revision 4

Majorite–olivine–high-Ca pyroxene assemblage in the shock-melt veins of Pervomaisky L6 chondrite

IVAN S. BAZHAN [1], KONSTANTIN D. LITASOV [1,2], EIJI OHTANI [1,3]
SHIN OZAWA [3]

[1] V.S. Sobolev Institute of Geology and Mineralogy SB RAS, Novosibirsk, 630090, Russia

[2] Novosibirsk State University, Novosibirsk, 630090, Russia

[3] Department of Earth and Planetary Materials Science, Graduate School of Science, Tohoku University, Sendai 980-8578, Japan

ABSTRACT

High-pressure minerals - majorite-pyrope garnet and jadeite - were found in the Pervomaisky L6 ordinary chondrite. Majorite-pyrope (79 mol% majorite) was observed within the fine-grained silicate matrix of a shock-melt vein (SMV), coexisting with olivine and high-Ca pyroxene. This is the first report of a garnet-olivine-high-Ca pyroxene assemblage that crystallized from the melt in the SMV matrix of meteorite. *PT*-conditions of the formation of the SMV matrix with olivine fragments are 13.5–15.0 GPa and 1750–2150 ^{o}C, the lowest parameters among all known majorite-bearing (H, L)-chondrites. The estimated conditions include the olivine/(olivine + ringwoodite) phase boundary and there is a possibility that observed olivine is the result of wadsleyite/ringwoodite back-transformation during a cooling and decompression stage. In the framework of this hypothesis, we discuss the problem of survival of the high-pressure phases at the post-shock stage in the meteorites and propose two possible *PT*-paths: (1) the high-pressure mineral is transformed to a low-pressure one during adiabatic decompression above the critical temperature of direct transformation; and (2) quenching below the critical temperature of direct transformation within the stability field of the high-pressure phase and further decompression. The aggregates with plagioclase composition ($Ab_{81.1}An_{14.9}Or_{4.1}$) occur in host-rock fragments near (or inside) of the SMV, and have a radial, concentric "spherulite-like" microstructure previously described in the Novosibirsk meteorite, and which is very similar to the texture of tissintite in the Tissint martian meteorite. It is likely that jadeite is related to crystallization of the SMV and could have formed from albitic feldspar (plagioclase) melt at 13.5–15.0 GPa and ~2000 °C.

Keywords: L6 chondrite Pervomaisky, olivine high-Ca pyroxene majorite-pyrope assemblage, jadeite, shock-melt vein history.

INTRODUCTION

Heavily shocked chondrites are unusual natural objects, containing a variety of assemblages of high-pressure polymorphs of rock-forming minerals (olivine, pyroxene and feldspar) formed by shock metamorphism during collisions of meteorite parent bodies. The shock events caused the melting of the host-rock, forming shock-melt veins (SMVs). The SMVs are the result of a combination of several processes: the compaction of pore space (e.g. Wünnemann et al. 2008), friction/shear heating (e.g. Langenhorst et al. 2002; Borgert et al. 2003) and localized stress and temperature at the interfaces of mineral grains (e.g. Stöffler et al. 1991). High-pressure and high-temperature phases in the shocked chondrites appear inside or near the SMVs.

Majorite is a high-pressure polymorph of pyroxene with garnet structure. Static experiments at high-pressure and high-temperature conditions indicate that the stability field of majorite in the system $MgO–SiO_2 \pm FeO \pm Al_2O_3$ is at about 15–23 GPa at temperatures above 1000 °C (e.g., Ringwood 1967; Ringwood and Major 1971; Akaogi and Akimoto 1977; Irifune 1987; Ohtani et al. 1991; Akaogi et al. 2002; Gasparik 2003). However, the formation of majorite-pyrope solid solutions related to pyroxene dissolution in a garnet structure begins at ~9 GPa (Ringwood 1967; Akaogi and Akimoto 1977).

Majorite-pyrope was found in SMV of L6 chondrite Coorara (Smith and Mason 1970) coexisting with ringwoodite. Majorite has been described in many shocked chondrites along with other high-pressure minerals, such as wadsleyite, ringwoodite, akimotoite, $MgSiO_3$-perovskite (bridgmanite), magnesiowüstite, lingunite, etc. (Price et al. 1979; Chen et al. 1996; Kimura et al. 2000; Xie et al. 2001; Kimura et al. 2003; Tomioka and Kimura 2003; Ohtani et al. 2004; Zhang et al. 2006; Ozawa et al. 2009; Miyahara et al. 2011; Acosta-Maeda et al. 2013; Tschauner et al. 2014).

Two types of majorite have been recognized. One forms by melting of the host rock and its crystallization under high-pressure conditions, forming the SMVs with other minerals (e.g., Smith and Mason 1970; Chen et al. 1996; Xie et al. 2001; Ohtani et al. 2004). This type of majorite is enriched in Al, Ca and Na compared with low-Ca pyroxene in the host-rock, and usually forms micron-size idiomorphic grains inside the matrix of the SMVs. Another type of majorite forms by a solid-state transformation of pyroxene in the coarse fragments of the host rock enclosed in the SMVs (Chen et al. 1996; Xie et al. 2001 Ohtani et al. 2004; Zhang et al. 2006; Xie and Sharp 2007). The chemical composition of such majorite is similar to that of pyroxene in the host rock.

The meteorite shower of the Pervomaisky L6 ordinary chondrite fell on the territory of Vladimir Region (Russia) on December 26, 1933 near Pervomaisky village. Pervomaisky belongs to the light-black species of chondrites (Britt and Pieters 1994). Semenenko and Golovko (1994) determined compositions of olivine, Ca-rich pyroxene, majorite-pyrope, feldspar, glass, chromite, whitlokite, kamacite and troilite, and they found organic matter (aliphatic hydrocarbons and carbonyl- and N-containing compounds) in the SMVs. Majorite-pyrope in Semenenko and Golovko (1994) was identified as Ca-poor pyroxene. No pressure estimation of majorite-pyrope formation conditions were reported. Later, Collerson et al. (2010) proposed a new majoritic barometer and estimated impact pressure in Pervomaisky as 21.9 GPa on the basis of the chemical composition of majorite-pyrope garnet published by Semenenko and Golovko (1994).

In this study, we conducted a detailed mineralogical investigation of the SMVs of the Pervomaisky L6 chondrite by scanning electron microscopy and micro-Raman spectrometry. As a result, we found high-pressure minerals jadeite and majorite-pyrope. The majorite-pyrope coexists with olivine and high-Ca pyroxene in the SMV matrix, which is an unusual assemblage for SMV matrix of chondrites. We discuss the conditions and the sequence of its formation.

MATERIALS AND METHODS

The sample of Pervomaisky was provided from the working collection of G. M. Ivanova (former scientific secretary of the Commission on Cosmic Meteorites and Dust at the Presidium of SB RAS). Sample preparation and investigation were done at the Department of Earth Science, Graduate School of Science, Tohoku University, Sendai, Japan. Petrologic observations were conducted using the polished chip samples under an optical microscope. Fine textural observations were conducted with the Field-Emission Scanning Electron Microscope (FE-SEM), JEOL JSM-7001F. Accelerating voltage and probe current were 15 kV and 1.4 nA, respectively. Chemical compositions of minerals were provided by the Energy-Dispersive X-ray Spectrometry (EDS) using an INCA Energy (Oxford Instruments) microanalysis system attached to the FE-SEM. Counting times for spectra collection were 30–60 seconds. Simple oxides - Al_2O_3 (for Al), MgO (for Mg); silicates - wollastonite, $CaSiO_3$ (for Si, Ca), albite, $NaAlSi_3O_8$ (for Na), orthoclase $KAlSi_3O_8$ (for K); metals – Cr, Ti, Fe, Mn, and GaP (for P), pyrite FeS_2 (for Fe, S) were used as the standards (see Lavrent'ev et al., 2015 for the details of the analytical procedure). Jadeite was additionally analysed by the area scan with shorter collection time (10-20 seconds) to minimize alkali loss during measurements.

Phase identification of minerals and glasses was conducted with the laser micro-Raman spectrometer, JASCO NRS-5100 (wavelength 532 nm). The laser power was 6.7 mW, and the size of the laser beam was ~1–2 μm in diameter. The Raman signal from the sample was collected for 60–120 seconds and accumulated twice for each point in the spectral range of 140–1206 cm^{-1}. Raman shift was calibrated with the peak of silicon standard at 520.5 ± 0.5 cm^{-1}.

RESULTS

The Pervomaisky chondrite belongs to the light-dark type of chondrites (Britt and Pieters, 1994). The light part was studied in this work. The host rock has an equilibrated chondrite texture and includes pervasive SMVs with widths of 10–300 μm (Fig. 1). The major constituent minerals of the host rock are olivine (Fa_{25}), low-Ca pyroxene ($En_{78}Fs_{21}Wo_{1}$), high-Ca pyroxene ($En_{47}Fs_{8}Wo_{45}$), maskelynite (former plagioclase) ($Ab_{83}An_{10.3}Or_{6.8}$) (Table 1), Fe-Ni metal, troilite, chromite and rare phosphates. Olivine, pyroxene and chromite are intersected by numerous, irregular cracks. All original plagioclase has been transformed to maskelynite. The SMVs consist of fine-grained silicate matrix with troilite and Fe-Ni metal blobs, and include coarse-grained fragments of the host-rock (Fig. 1b). The chemical compositions of olivine and pyroxene in the fragments are almost identical to those in the host rock (Table 1). The analyses of maskelynite show low totals, which may be related to the deficit of Na_2O due to partial volatile loss under the electron beam. We performed corrections of Na contents in previous experimental work (Shatskiy et al., 2013a,b). A maskelynite analysis with a corrected Na_2O content is shown in Table 1.

The Raman spectra of the SMV matrix contain peaks corresponding to majorite-pyrope (at ~928 cm^{-1}), olivine (at ~822 and ~855 cm^{-1}) and high-Ca pyroxene (broad peaks at ~668 and ~1014 cm^{-1}) (spectrum R1 in Fig. 2). Olivine and high-Ca pyroxene peaks are present in all spectra containing majorite-pyrope peaks. There are probably micron-sized majorite-pyrope grains submerged the mixture of submicron olivine and high-Ca pyroxene grains, and it is impossible to get Raman spectra only with garnet peaks due to the larger diameter (~2 μm) of the Raman laser beam.

Majorite-pyrope occurs as idiomorphic grains with sizes up to 3 μm (Fig. 1c). The largest grains occur in the central parts of the SMVs. The average composition of majorite-pyrope is $Na_{0.07}Ca_{0.19}Mg_{2.90}Mn_{0.03}Fe_{0.72}Cr_{0.02}Al_{0.41}Si_{3.77}O_{12}$. It corresponds to about 79 mol% of majorite component in the majorite-pyrope solid solution. Majorite-pyrope is enriched in Al_2O_3 (4.68–5.10 wt%), CaO (2.16–2.75 wt%) and Na_2O (0.45–0.59 wt%) relative to low-Ca pyroxene in the host-rock (0.18–0.26 wt% Al_2O_3; 0.43–0.94 wt% CaO) (Table 1). In the centers of the SMVs (Figs. 1d and 1e), we found black, rounded, fine grains up to 5 μm and light interstitial material between them (Fig. 1e). The FE-SEM-EDS analyses obtained from the center of a zoned grain (Fig. 1e) shows high-Ca pyroxene composition $Na_{0.05}Ca_{0.70}Mg_{1.04}Mn_{0.01}Fe_{0.19}Cr_{0.02}Al_{0.05}Ti_{0.01}Si_{1.95}O_6$ ($En_{53.8}Fs_{9.6}Wo_{36.6}$). Light grains interstitial to the black grains (Fig. 1e) have olivine (Fa_{25-35}) composition. Magnesiowüstite and high-pressure polymorphs of olivine were not found in Pervomaisky.

We identified plagioclase-composition aggregates with jadeite (jadeite aggregates) as 5–20 μm fragments in the SMVs (Figs. 1b and 1c). Jadeite aggregates are slightly enriched in Fe, Ca and Na and depleted in K compared with maskelynite (Table 1). All jadeite aggregates have radial, concentric, "spherulite-like" microstructures, which are similar to those previously described in jadeite aggregates from the Novosibirsk meteorite (Bazhan et al. 2017). The Raman spectra obtained from the jadeite aggregate (peaks at ~1038, ~699, ~579, ~526 and ~379 cm^{-1}) also include peaks of majorite-pyrope (at ~928 cm^{-1}), olivine (at ~823 and ~855 cm^{-1}) and a small peak of high-Ca pyroxene (at ~665 cm^{-1}) (spectrum R2 in Fig. 2). Raman peaks of majorite-pyrope, olivine and high-Ca pyroxene in jadeite spectrum appears from the surrounding minerals.

DISCUSSION

PT-conditions for SMV formation in the Pervomaisky meteorite

The shock event caused melting of the chondrite, forming the SMVs. The growth of majorite-pyrope grains could occur during a cooling stage after crystallization and quenching of olivine–high-Ca pyroxene melt portion. *P-T* conditions of SMV formation in Pervomaisky can be obtained from the phase assemblage of majorite-pyrope + olivine + high-Ca pyroxene in the SMV matrix. The phase diagrams of the $CaO-MgO-Al_2O_3-SiO_2$ (CMAS) system (Fig.6 in Gasparik 1996) show that this assemblage can be stable at 7–16 GPa and 500–2150 °C. The stability field of the present assemblage is limited to 14–15 GPa and 1750–2150 °C due to its content of 79 mol% majorite component in majorite-pyrope garnet (Fig. 6 in Gasparik 1996).

The estimated *P-T* conditions are higher than the stability field of olivine (Fa_{25}) in the host-rock fragments in the SMV. Olivine should have transformed to its high-pressure polymorphs (wadsleyite and ringwoodite), according to the relevant phase diagram (Fig. 3; Akaogi et al. 1989). However, these phases are not found in Pervomaisky. To explain this discrepancy we propose two possibilities: (1) the pressure was lower than estimated; and (2) wadsleyite/ringwoodite back-transformed to olivine during a cooling + decompression stage.

The upper limit of *P*-*T* stability of olivine fragments (Fa_{25}; Table 1) in the SMV would be ~13.5 GPa and ~2150 ^{o}C, which is at the intersection of olivine/(olivine + ringwoodite) transition line (from Akaogi et al., 1989) and the liquidus curve of olivine in the melting phase diagrams of anhydrous peridotite KLB-1 (Zhang and Herzberg 1994; Fig. 3). The estimated pressure for the SMV matrix assemblage formation (~14–15 GPa) and the upper pressure limit for olivine survival in the fragments (~13.5 GPa) are very close and do not contradict each other. According to the static kinetic experiments of olivine-wadsleyite transformations (e.g. Kubo et al. 2004), micron-size grains of wadsleyite appear after several minutes in experiments at 13.6–15.6 GPa and 1000–1100 ^{o}C. The overpressure range at these conditions was 0.3–2.5 GPa (Kubo et al. 2004). Thus, we suggest that the pressure range of the SMV mineral assemblage in Pervomaisky is 13.5–15.0 GPa.

The majoritic barometer (Collerson et al. 2010) gives pressure estimations of 21 and 22 GPa, using the present and the Semenenko and Golovko (1994) majorite-pyrope compositions (Table 1), respectively. It can be argued that the majoritic barometer from Collerson et al. (2010) does not consider mineral assemblages and may overestimate pressures. For example, in the pressure-composition phase diagram (Gasparik 2003; Fig. 4), it can be shown that the same chemical composition (i.e., 79 mol% of majorite in Pervomaisky) corresponds to five different assemblages at different pressures.

We think that our pressure estimations of 13.5–15.0 GPa for Pervomaisky are more reliable than the 21 GPa of Collerson et al. (2010), because at such high pressure, wadsleyite or ringwoodite should be present. We plotted pressure estimations versus pyrope contents in majorite-pyrope garnet for different chondrites (Fig. 4). The *P*-*T* conditions for shock vein formation in Pervomaisky are the lowest among all known majorite-bearing H- and L- chondrites (Table 2, Fig. 4).

The back-transformations of high-pressure minerals to low pressure phases in shocked chondrites

We could not avoid the fact that the estimated conditions (13.5–15.0 GPa) include the olivine/(olivine + ringwoodite) phase boundary and there is a possibility that olivine in the fragments is the result of wadsleyite/ringwoodite back-transformation during a cooling-decompression stage. For example, Kimura et al. (2003) reported the back-transformations of the high-pressure minerals in a SMV (ringwoodite, wadsleyite, akimotoite, and majorite) to the low-pressure polymorphs as a result of secondary external heating (up to 1600 °C) of the SMV close to the fusion crust during the atmospheric passage of Yamato 75267 meteorite. The estimated time of the back-transformation in Yamato 75267 was several seconds (Kimura et al. 2003). In addition, Chen et al. (1998) showed that the back-transformation depends on the cooling rate. It was found that no back-transformation of ringwoodite to olivine and majorite to pyroxene in the Sixiangkou meteorite occurred at the cooling rate >10000 °C/s. The partial back-transformation of the same minerals occurred in the Peace River meteorite at the cooling rate of 1000–2000 °C/s and the transformation was mostly completed at cooling rate <500 °C/s in the Mbale meteorite.

The finding of the back-transformation features of high-pressure minerals in the meteorites, such as iron zoning in olivine grain as relics of wadsleyite/ringwoodite crystallization from the melt in Mbale (Chen et al. 1998), remnant features of polycrystalline grain boundary nucleation and intracrystalline ringwoodite lamellae formation, or sharp boundaries between areas containing low-pressure and high-pressure minerals (Kimura et al. 2003), are difficult to detect. We did not find clear evidence of the back-transformation of olivine high-pressure polymorphs in Pervomaisky.

PT-paths for the survival or back-transformation of ringwoodite and wadsleyite

The experimental data of Nishi et al. (2010) show that the time required for the back transformation of majorite to pyroxene is longer than previously reported (Kimura et al. 2003; Chen et al. 1998). According to their data, the growth of 5 μm grains of high-Ca pyroxene during back transformation of majorite at 7 GPa and 1100 °C takes 150 minutes. This is significantly longer relative to the duration of the impact events in different chondrites, which was estimated as 0.04–4 seconds (Ohtani et al. 2004; Beck et al. 2005; Xie et al. 2006). The absence of ringwoodite and wadsleyite and survival of majorite-pyrope in the meteorite are probably related to the different kinetics of the back-transformations of these minerals during the post-shock period of time at rapid decompression and relatively slow cooling of the SMV, i.e. adiabatic decompression stage. In Figure 3, a solid arrow (path 1) schematically shows this scenario.

The preservation of metastable phases during pressure and temperature release from initial shock conditions requires quenching below the breakdown temperature before complete pressure release (Sharp et al. 2003, Ohtani et al. 2004). Suzuki et al. (1980) noticed that wadsleyite (β-Mg_2SiO_4) promptly transforms to olivine at 900 ^oC and ambient pressure. Ming et al. (1991) showed that ringwoodite (Mg_2SiO_4) transforms to olivine in 1.3 h at the same *P-T* condition. Their studies suggest that a temperature of 900 ^oC would be a critical threshold for the survival of high-pressure polymorphs of olivine in the chondrites at the cooling-decompression stage, when they passed through the metastable pressure range. In Figure 3, a dashed arrow (path 2) schematically shows this scenario. The transformation of ringwoodite/wadsleyite to olivine occurs quickly during adiabatic decompression above 900 ^oC (path 1 in Fig.3).

Jadeite chemical composition and texture

The chemical composition of jadeite aggregates in Pervomaisky is closer to plagioclase stoichiometry than that of jadeite (Table 1). It is related to silica excess in jadeite compositions and was reported previously for many jadeite-bearing chondrites (e.g. Kimura et al. 2000; Zhang et al. 2006; Ozawa et al. 2009, 2014; Miyahara et al. 2013; Bazhan et al. 2017). Silica accompanies jadeite formation by plagioclase (albite) dissociation reaction: albite = jadeite + silica at pressures above 3 GPa and 1000 ^{o}C (Birch and LeComte 1960; Bell and Roseboom Jr 1969; Liu 1978; Holland 1980). Kubo et al. (2010) and Miyahara et al. (2013) provided detailed investigations of jadeite formation from albite in experiments and in chondrites, respectively. Kubo et al. (2010) suggested that amorphous plagioclase breaks down into jadeite and SiO_2 at high temperatures and pressures, and nucleation of SiO_2 (stishovite) is significantly delayed compared with jadeite. Miyahara et al. (2013) studied jadeite-bearing chondrites and found that areas containing jadeite consist of two phases: jadeite + residual amorphous material. The average SiO_2 contents in jadeites recovered from the chondrite samples Y-791384 and Y-75100 (Miyahara et al. 2013) and from the synthetic sample s1644 (Kubo et al. 2010) are 61.2 wt%, 61.8 wt%, and 57.4 wt% respectively. Apparently, the excess of SiO_2 in the chemical composition of jadeite in Pervomaisky (65.7 wt% Table 1), is also associated with the presence of SiO_2-rich microinclusions.

The textures of "spherulite-like" jadeite aggregates in Pervomaisky (Fig. 1c) and Novosibirsk (H5/6) (Bazhan et al. 2017) chondrites appear to be very similar to each other, with wormy and rimming textural forms of tissintite, - vacancy-rich, high-pressure clinopyroxene $(Ca,Na,\square)AlSi_2O_6$ recently reported in the Tissint Martian meteorite (Ma et al. 2015), but are different in chemical compositions. The composition of jadeite in Pervomaisky and Novosibirsk correspond to An_{15} and An_{14}, respectively, whereas tissintite from Tissint is $An_{58-69.}$ Jadeite and tissintite aggregates with new textures were found in maskelynite enclosed by, or within ~25 μm of, a shock melt vein/pocket. Ma et al. (2015) proposed two main possibilities of tissintite formation during an impact event via crystallization from a plagioclase melt: (1) as a stable liquidus phase; and (2) as a subliquidus phase due to enhanced nucleation rates. According to Ma et al. (2015), the distance of

~25 μm could be critical to tissintite formation. The grains of maskelynite located more than ~25 μm from a melt pocket either did not melt or were not heated sufficiently to allow for tissintite crystallization. The second option is similar to that proposed by Bazhan et al. (2017) for "spherulite-like" jadeite in the Novosibirsk chondrite. They assumed that "spherulite-like" texture of jadeite is the result of nucleation and growth of submicron jadeite crystals from plagioclase melt along the grain boundary with surrounding minerals (olivine and high-Ca pyroxene). "Spherulite-like" jadeite in Pervomaisky and Novosibirsk and wormy and rimming tissintite in Tissint are not the same mineral, since they have different Raman spectra and chemical compositions, Tissintite could be formed only from a Ca-rich plagioclase melt ($>An_{33}$), and is unlikely to be found in ordinary chondrites (like Pervomaisky) with Na-rich plagioclase (Ma et al. 2015). Despite these differences, they have similar formation mechanisms, *P-T* conditions and aggregate textures.

PT-condition of jadeite formation

The minimum pressure of albite dissociation reaction to jadeite + silica is 3 GPa (Birch and LeComte 1960; Bell and Roseboom Jr 1969; Liu 1978; Holland 1980). The silica phase changes from quartz to coesite and stishovite with increasing pressure. At pressures of 19–23 GPa, the jadeite + stishovite assemblage transforms to lingunite ($NaAlSi_3O_8$-hollandite) or to $NaAlSiO_4$ (with $CaFeO_4$-type structure) + stishovite (Tutti 2007). Thus, the pressure range of jadeite stability is 3–19 GPa (Fig. 3; Ozawa et al. 2014).

Two types of jadeite have appeared in shocked meteorites. The first one has a chemical composition which is nearly identical to albitic feldspar (plagioclase), maskelynite or lingunite in the host-rocks or in the host-rock fragments in SMVs, and forms through a solid-state transformation (sst) of these phases (Ozwa et al., 2009; Miyahara et al., 2013). The SMVs of chondrites containing this type of jadeite (Jd_{sst}) also include majorite-pyrope, wadsleyite, ringwoodite and akimotoite (Table 2). The *P-T* fields of Jd_{sst} in Figure 3 are Jd_{sst}+Sti and Jd_{sst}+Coe, and correspond to the *PT*-fields of majorite-pyrope, wadsleyite, and ringwoodite. The Jd_{sst} formation does not contradict the survival of the high-pressure minerals by path 2 in Figure 3.

The composition of the second type of jadeite is different from that of plagioclase in the host-rocks and forms from albite melt slightly contaminated by surounding silicates (Jd_{melt}; Fig.3). Although it is not clearly seen from melt pocket images, jadeite is always accompanied by tiny amorphous SiO_2-bearing residue and has high-SiO_2 contents (e.g. Miyahara et al., 2013). Jadeite in Pervomaisky belongs to this type and is similar to that in the Chelyabinsk (Ozawa et al. 2014) and Novosibirsk (Bazhan et al. 2017) chondrites. Jadeite in Pervomaisky could have formed at 13.5–15.0 GPa and ~ 2000 ^{o}C, as shown in Fig. 3, in the beginning of cooling stage of the paths 1 and 2.

IMPLICATIONS

We propose two possible scenarios (*PT*-paths) for olivine fragments found in majorite-pyrope-bearing SMV silicate matrix using the KLB-1 peridotite melting phase diagram with the boundaries of olivine and albite high-pressure phases (Fig. 3). Path 1 characterizes the history of mineral formation/transformation during cooling and adiabatic decompression stages (Fig. 3). A hypothetical ringwoodite/wadsleyite + majorite-pyrope + high-Ca pyroxene assemblage would form from chondrite melt at 14–15 GPa and 1750–2150 ^{o}C at cooling of the SMVs with subsequent jadeite formation in plagioclase-bearing melt pockets. The back-transformation of ringwoodite/wadsleyite to olivine (in the fragments and in the SMV matrix) could occur during an adiabatic decompression stage at the end of path 1 (Fig. 3). The survival of majorite-pyrope can be explained by the different kinetics of the back-transformation of ringwoodite/wadsleyite to olivine and majorite-pyrope to pyroxene. The survival of ringwoodite/wadsleyite could occur along path #2 that is an extension of the cooling stage of path #1 below 900 ^{o}C and excludes the adiabatic stage

(Fig. 3). Whether jadeite formed from the melt or by the solid-state transformation of plagioclase depends on the shock temperature and is consistent with both scenarios (Fig. 3). The SMVs in the Mbale chondrite (Chen et al. 1998) would have evolved along the *PT*-path #1, whereas those of Tenham, Y-75100, Suizhou, Y-75267, Y-791384, Sixiangkou, Y-74445, Taiban and Sahara 98222 correspond to the *PT*-path #2.

We suggest that our pressure estimation (13.5–15.0 GPa) for majorite-pyrope assemblage formation in the SMV of Pervomaisky is the lowest among known majorite-bearing chondrites. To our knowledge, this is the first report of the coexistence of highly majoritic garnet with olivine and high-Ca pyroxene in the SMV matrix of chondrites.

ACKNOWLEDGMENTS

We thank S. Simon and two anonymous reviewers for constructive comments and G.M. Ivanova and N.M. Podgornykh for providing samples of the Pervomaisky meteorite. The authors are also grateful to Y. Ito for preparation and chemical analyses of meteorite samples. The work was conducted under the program of Ministry of Education and Science of Russian Federation (No 14.B25.31.0032). KL thanks to support of his research from Russian Science Foundation (project No 15-17-30012).

REFERENCES

Acosta-Maeda, T.E., Scott, E.R.D., Sharma, S.K., and Misra, A.K. (2013) The pressures and temperatures of meteorite impact: Evidence from micro-Raman mapping of mineral phases in the strongly shocked Taiban ordinary chondrite. American Mineralogist, 98, 859–869.

Akaogi, M., and Akimoto, S. (1977) Pyroxene-garnet solid-solution equilibria in the systems $Mg_4Si_4O_{12}$–$Mg_3Al_2Si_3O_{12}$ and $Fe_4Si_4O_{12}$–$Fe_3Al_2Si_3O_{12}$ at high pressures and temperatures. Physics of the Earth and Planetary Interiors, 15, 90–106.

Akaogi, M., and Navrotsky, A. (1984) The quartz-coesite-stishovite transformations: new calorimetric measurements and calculation of phase diagrams. Physics of the Earth and Planetary Interiors, 36, 124-134.

Akaogi, M., Ito, E., and Navrotsky, A. (1989) Olivine-modified spinel-spinel transitions in the system Mg_2SiO_4–Fe_2SiO_4: Calorimetric measurements, thermochemical calculation, and geophysical application. Journal of Geophysical Research, 94, 15671–15685.

Akaogi, M., Tanaka, A., and Ito, E. (2002) Garnet-ilmenite-perovskite transitions in the system $Mg_4Si_4O_{12}$–$Mg_3Al_2Si_3O_{12}$ at high pressures and high temperatures: phase equilibria, calorimetry and implications for mantle structure. Physics of the Earth and Planetary Interiors, 132(4), 303–324.

Bazhan, I., Ozawa, S., Ohtani, E., and Litasov, K. (2017) “Spherulite-like” jadeite in shocked H5/6 chondrite Novosibirsk. Russian Geology and Geophysics, 58 (1), 12–19.

Birch, F., and LeComte, P. (1960). Temperature-pressure plane for albite composition. American Journal of Science, 258, 209–217.

Beck, P., Gillet, P., El Goresy, A., and Mostefaoui, S. (2005) Timescales of shock processes in chondritic and martian meteorites. Nature, 435, 1071–1074.

Bell, P. M., and Roseboom Jr, E. H. (1969) Melting relationships of jadeite and albite to 45 kilobars with comments on melting diagrams of binary systems at high pressures. Mineralogical Society of America Special Paper, 2, 151–169.

Britt, D., and Pieters, C. (1994) Darkening in black and gas-rich ordinary chondrites: The spectral effects of opaque morphology and distribution. Geochimica et Cosmochimica Acta, 58, 3905–3919.

Chen, M., Sharp, T.G., El Goresy, A., Wopenka, B., and Xie, X. (1996) The majorite-pyrope+ magnesiowüstite assemblage: Constraints on the history of shock veins in chondrites. Science, 271, 1570–1573.

Chen, M., Xie, X., El Goresy, A., Wopenka, B., and Sharp, T. (1998) Cooling rates in the shock veins of chondrites: constraints on the $(Mg,Fe)_2SiO_4$ polymorph transformations. Science in China Series D: Earth Sciences, 41, 522–528.

Collerson, K.D., Williams, Q., Kamber, B.S., Omori, S., Arai, H., and Ohtani, E. (2010) Majoritic garnet: A new approach to pressure estimation of shock events in meteorites and the encapsulation of sub-lithospheric inclusions in diamond. Geochimica et Cosmochimica Acta, 74, 5939–5957.

Gasparik, T. (1996) Melting experiments on the enstatite-diopside join at 70–224 kbar, including the melting of diopside. Contributions to mineralogy and petrology, 124, 139–153.

Gasparik, T. (2003) Phase diagrams for geoscientists. An Atlas of the Earth's Interior. 2nd ed., Springer, 462 p.

Holland, T.J.B. (1980) The reaction albite= jadeite+ quartz determined experimentally in the range 600-1200 ^{o}C. American Mineralogist, 65, 129–134.

Irifune, T. (1987) An experimental investigation of the pyroxene-garnet transformation in a pyrolite composition and its bearing on the constitution of the mantle. Physics of the Earth and Planetary Interiors, 45, 324–336.

Kimura, M., Suzuki, A., Kondo, T., Ohtani, E., and El Goresy, A. (2000) Natural occurrence of high-pressure phases, jadeite, hollandite, wadsleyite and majorite-pyrope garnet, in an H-chondrite, Y75100. Meteorit. Planet. Sci., 35, 87–88.

Kimura, M., Chen, M., Yoshida, Y., El Goresy, A., and Ohtani, E. (2003) Back-transformation of high-pressure phases in a shock melt vein of an H-chondrite during atmospheric passage: Implications for the survival of high-pressure phases after decompression. Earth and Planetary Science Letters, 217, 141–150.

Kubo, T., Ohtani, E., and Funakoshi, K (2004). Nucleation and growth kinetics of the α-β transformation in Mg_2SiO_4 determined by in situ synchrotron powder X-ray diffraction. American Mineralogist, 89, 285–293.

Kubo, T., Kimura, M., Kato, T., Nishi, M., Tominaga, A., Kikegawa, T., and Funakoshi, K. (2010) Plagioclase breakdown as an indicator for shock conditions of meteorites. Nature Geoscience, 3, 41–45.

Langenhorst, F., Joreau, P., and Doukhan, J. C. (1995) Thermal and shock metamorphism of the Tenham chondrite: A TEM examination. Geochimica et Cosmochimica Acta, 59, 1835–1845.

Langenhorst, F., Poirier, J.-P., Deutsch, A., and Hornemann, U. (2002) Experimental approach to generate shock veins in single-crystal olivine by shear melting. Meteoritics & Planetary Science, 37, 1541–1553.

Lavrent'ev, Y. G., Karmanov, N.S, and Usova, L.V., 2015. Electron probe microanalysis of minerals: Microanalyzer or scanning electron microscope? Russian Geology and Geophysics, 56, 1154–1161.

Liu, L.-G. (1978) High-pressure phase tranformations of albite, jadeite and nepheline. Earth and Planetary Science Letters, 37, 438–444.

Ma, C., Tschauner, O., Beckett, J. R., Liu, Y., Rossman, G. R., Zhuravlev, K., and Taylor, L. A. (2015) Tissintite, (Ca,Na, □)$AlSi_2O_6$, a highly-defective, shock-induced, high-pressure clinopyroxene in the Tissint martian meteorite. Earth and Planetary Science Letters, 422, 194–205.

Ming, L., Kim, Y., Manghnani, M., Usha-Devi, S., Ito, E., and Xie, H.-S. (1991) Back-transformation and oxidation of $(Mg,Fe)_2SiO_4$ spinels at high temperatures. Physics and chemistry of minerals, 18, 171–179.

Miyahara, M., Ohtani, E., Kimura, M., Ozawa, S., Nagase, T., Nishijima, M., and Hiraga, K. (2011) Evidence for multiple dynamic events and subsequent decompression stage recorded in a shock vein. Earth and Planetary Science Letters, 307, 361–368.

Miyahara, M., Ozawa, S., Ohtani, E., Kimura, M., Kubo, T., Sakai, T., Nagase, T., Nishijima, M., and Hirao, N. (2013) Jadeite formation in shocked ordinary chondrites. Earth and Planetary Science Letters, 373, 102–108.

Nishi, M., Kubo, T., Kato, T., Tominaga, A., Shimojuku, A., Funakoshi, K., and Higo, Y. (2010). Survival of majoritic garnet in diamond by direct kimberlite ascent from deep mantle. Geophysical Research Letters, 37, L09305.

Ohtani, E., Kagawa, N., and Fujino, K. (1991) Stability of majorite $(Mg,Fe)SiO_3$ at high pressures and 1800° C. Earth and Planetary Science Letters, 102, 158–166.

Ohtani, E., Kimura, Y., Kimura, M., Takata, T., Kondo, T., and Kubo, T. (2004) Formation of high-pressure minerals in shocked L6 chondrite Yamato 791384: constraints on shock conditions and parent body size. Earth and Planetary Science Letters, 227, 505–515.

Ozawa, S., Ohtani, E., Miyahara, M., Suzuki, A., Kimura, M., and Ito, Y. (2009) Transformation textures, mechanisms of formation of high-pressure minerals in shock melt veins of L6 chondrites, and pressure-temperature conditions of the shock events. Meteoritics & Planetary Science, 44, 1771–1786.

Ozawa, S., Miyahara, M., Ohtani, E., Koroleva, O., Ito, Y., Litasov, K., and Pokhilenko, N. (2014) Jadeite in Chelyabinsk meteorite and the nature of an impact event on its parent body. Scientific Reports, 4, 5033.

Price, G., Putnis, A., and Agrell, S. (1979) Electron petrography of shock-produced veins in the Tenham chondrite. Contributions to Mineralogy and Petrology, 71, 211–218.

Ringwood, A.E. (1967) The pyroxene-garnet transformation in the earth's mantle. Earth and Planetary Science Letters, 2, 255–263.

Ringwood, A.E., and Major, A. (1971) Synthesis of majorite and other high pressure garnets and perovskites. Earth and Planetary Science Letters, 12, 411–418.

Semenenko, V., and Golovko, N. (1994) Shock-induced black veins and organic compounds in ordinary chondrites. Geochimica et Cosmochimica Acta, 58, 1525–1535.

Sharp, T., Xie, Z., Aramovich, C., and De Carli, P. (2003) Pressure-temperature histories of shock-induced melt veins in chondrites. Lunar and Planetary Science Conference, 34, 1278.

Shatskiy, A., Gavryushkin, P. N., Sharygin, I. S., Litasov, K. D., Kupriyanov, I. N., Higo, Y., and Ohtani, E. (2013a). Melting and subsolidus phase relations in the system Na_2CO_3-$MgCO_3$±H_2O at 6 GPa and the stability of $Na_2Mg\ (CO_3)_2$ in the upper mantle. American Mineralogist, 98, 2172–2182.

Shatskiy, A., Sharygin, I. S., Litasov, K. D., Borzdov, Y. M., Palyanov, Y. N., and Ohtani, E. (2013b). New experimental data on phase relations for the system Na_2CO_3-$CaCO_3$ at 6 GPa and 900–1400 ºC. American Mineralogist, 98, 2164–2171.

Smith, J.V., and Mason, B. (1970) Pyroxene-garnet transformation in Coorara meteorite. Science, 168, 832–833.

Suzuki, I., Ohtani, E., and Kumazawa, M. (1980) Thermal expansion of modified spinel, beta-Mg_2SiO_4. Journal of Physics of the Earth, 28, 273–280.

Stöffler, D., Keil, K., and Scott, E.R.D. (1991) Shock metamorphism of ordinary chondrites. Geochimica et Cosmochimica Acta, 55, 3845–3867.

Tomioka, N., and Fujino, K. (1999) Akimotoite, $(Mg,Fe)SiO_3$, a new silicate mineral of the ilmenite group in the Tenham chondrite. American Mineralogist, 84, 267–271.

Tomioka, N., and Kimura, M. (2003) The breakdown of diopside to Ca-rich majorite and glass in a shocked H chondrite. Earth and Planetary Science Letters, 208, 271–278.

Tschauner, O., Ma, C., Beckett, J.R., Prescher, C., Prakapenka, V.B., and Rossman, G.R. (2014) Discovery of bridgmanite, the most abundant mineral in Earth, in a shocked meteorite. Science, 346, 1100–1102.

Tutti, F. (2007) Formation of end-member $NaAlSi_3O_8$ hollandite-type structure (lingunite) in diamond anvil cell. Physics of the Earth and Planetary Interiors, 161, 143–149.

van der Bogert, C.H., Schultz, P.H., and Spray, J.G. (2003) Impact-induced frictional melting in ordinary chondrites: A mechanism for deformation, darkening, and vein formation. Meteoritics & Planetary Science, 38, 1521–1531.

Xie, X., Chen, M., and Wang, D. (2001) Shock-related mineralogical features and PT history of the Suizhou L6 chondrite. European Journal of Mineralogy, 13, 1177–1190.

Xie, X., Minitti, M. E., Chen, M., Mao, H.-K., Wang, D., Shu, J., and Fei, Y. (2003). Tuite, γ-$Ca_3(PO4)_2$: A new mineral from the Suizhou L6 chondrite. European Journal of Mineralogy, 15(6), 1001-1005. Xie, Z.D., Sharp, T.G., and DeCarli, P.S. (2006) High-pressure phases in a shock-induced melt vein of the Tenham L6 chondrite: Constraints on shock pressure and duration. Geochimica et Cosmochimica Acta, 70, 504–515.

Xie, Z., and Sharp, T.G. (2007) Host rock solid-state transformation in a shock-induced melt vein of Tenham L6 chondrite. Earth and Planetary Science Letters, 254, 433–445.

Wünnemann, K., Collins, G., and Osinski, G. (2008) Numerical modelling of impact melt production in porous rocks. Earth and Planetary Science Letters, 269, 530–539.

Zhang, J., and Herzberg, C. (1994) Melting experiments on anhydrous peridotite KLB-1 from 5.0 to 22.5 GPa. Journal of Geophysical Research: Solid Earth, 99, 17729–17742.

Zhang, A.C., Hsu, W.B., Wang, R.C., and Ding, M.W. (2006) Pyroxene polymorphs in melt veins of the heavily shocked Sixiangkou L6 chondrite. European Journal of Mineralogy, 18, 719–726.

Table and Figure captions

Table 1. Average chemical compositions of the minerals of the Pervomaisky chondrite.

Table 2. High-pressure mineral assemblages in different chondrites.

Figure 1. Back-scattered electron images of the Pervomaisky L6 chondrite. (**a**) a shock-melt vein (SMV) that cuts the host rock; (**b**) a SMV with an entrained host rock fragment; (**c**) an aggregate of jadeite in a SMV silicate matrix; R1, R2 and R3 in (c) indicate points where the Raman spectra in Fig. 2 were obtained; (**d**) the matrix of the SMV with majorite-pyrope – olivine – high-Ca pyroxene assemblage; (**e**) magnified image of the area marked by a rectangle in (d). Cpx, high-Ca pyroxene; En, enstatite; Fa, fayalite; Fs, ferrosilite; Jd, plagioclase composition aggregate with jadeite; Maj-Prp, majorite-pyrope; Msk, maskelynite; Ol, olivine; Opx, low-Ca pyroxene; Tro, troilite, Wo, wollastonite.

Figure 2. Representative Raman spectra from different points of fine-grained silicate matrix of the SMV of the Pervomaisky chondrite. Analytical points (R1 and R2) are marked in Figure 1c. R1 spectrum from - majorite-pyrope – olivine – high-Ca pyroxene assemblage. R2 spectrum from jadeite aggregate. Cpx, high-Ca pyroxene; Jd, jadeite; Maj-Pyr, majorite-pyrope; Ol, olivine.

Figure 3. *PT*-conditions for majorite-pyrope + olivine + high-Ca pyroxene assemblage formation (dark grey bar) in the SMV of the Pervomaisky chondrite. Liquidus and solidus of KLB-1 peridotite are from Zhang and Herzberg (1994); Black bold lines represent phase boundaries for olivine (Fa_{25}) (Akaogi et al. 1989) in Pervomaisky. Grey lines represent phase boundaries for albite (after Bell and Roseboom 1969; Akaogi and Navrotsky 1984; Tutti 2007; Ozawa et al. 2014). Light grey area is stability field of jadeite. The solid arrow #1 schematically shows a possible *PT*-path of the back-

transformation of ringwoodite and wadsleyite to olivine in Pervomaisky at the post-shock, adiabatic decompression stage. The dashed arrow #2 schematically shows a possible *P*-*T* path of the survival of ringwoodite and wadsleyite in chondrite in a post-shock, cooling-decompression stage. Transition temperature from ringwoodite/wadsleyite to olivine at ambient pressure is 900 ^{o}C (see text). Ab, albite, Coe, Coesite; Grt, garnet (majorite-pyrope); Jd, jadeite; Jd_{melt}, jadeite formed from the melt; Jd_{sst}, jadeite formed by solid-state transformation (SST) of albite; L_{Ab}, albite melt; Lng, lingunite; Mws, magnesiowüstite; Ol, olivine; Qz, quartz; Rwd, ringwoodite, Sti, stishovite; Wds, wadsleyite.

Figure 4. A portion of the P-X phase diagram for the enstatite-diopside-pyrope garnet join and for a pyrope content of 0-30 mol% at 1650 ^{o}C (Fig. 3.9 in Gasparik 2003). The bars show pyrope/majorite content in majorite-pyrope garnets in the SMVs and pressure estimation of high-pressure mineral assemblage formation in different chondrites (Table 2): (1) Pervomaisky (Present study); (2) Suizhou (Xie et al. 2001); (3) Sixiangkou (Zhang et al. 2006); (4) Yamato 791384 (Ohtani et al. 2004); (5) Yamato 75100 (Tomioka et al. 2003); (6) Yamato 75267 (Kimura et al. 2003); (7) Tenham (Langenhorst et al. 1995); (8) Tenham (Tomioka and Kimura 1999).

TABLE 1. Average chemical compositions of the minerals of the Pervomaisky chondrite

oxides wt%	Ol			Cpx		Opx		Melt	Maj-Prp	Opx$_{Sem}$		Msk	Jd
	h-rock	fragm		h-rock	fragm	h-rock	fragm	vein	vein	vein		h-rock	fragm
n	12	7		11	7	24	14	5	3	6		4	4
SiO_2	38.3(5)	38.1(5)		54.4(6)	54.5(4)	55.5(6)	55.9(8)	48.9(2.0)	52.9(41)	52.9		65.9(6)	65.7(5)
TiO_2	n.d.	n.d.		0.46(6)	0.51(10)	b.d.	b.d.	b.d.	b.d.	0.14		n.d.	-
Al_2O_3	n.d.	n.d.		0.52(8)	0.55(9)	b.d.	b.d.	3.12(38)	4.91(21)	2.56		20.7(3)	20.3(5)
Cr_2O_3	n.d.	n.d.		0.83(11)	0.82(11)	n.d.	n.d.	0.31(7)	0.43(13)	0.54		n.d.	-
FeO	22.7(1)	22.7(6)		5.11(42)	5.43(13)	13.9(5)	14.4(1)	15.2(3)	12.0(1.0)	11.0		0.79(18)	1.56(9)
NiO	n.d.	n.d.		n.d.	n.d.	n.d.	n.d.	b.d.	b.d.	n.d.		n.d.	-
MnO	0.49(11)	0.45(5)		b.d.	b.d.	0.52(9)	0.54(7)	0.35(13)	0.47(5)	0.33		n.d.	-
MgO	38.6(6)	38.9(7)		16.7(2)	16.8(3)	28.8(5)	29.0(3)	29.6(2.2)	26.7(72)	29.6		b.d.	0.30(11)
CaO	n.d.	n.d.		21.9(6)	21.5(3)	0.72(13)	0.65(12)	2.10(57)	2.55(34)	1.88		1.78(8)	2.40(9)
Na_2O	n.d.	n.d.		0.56(9)	0.54(3)	n.d.	n.d.	0.48(28)	0.51(7)	0.29		7.94	9.52(42)
K_2O	n.d.	n.d.		n.d.	n.d.	n.d.	n.d.	b.d.	n.d.	n.d.		0.99(5)	0.62(8)
Total	100.09	100.15		100.48	100.65	99.44	100.49	100.06	100.47	99.24		98.11	100.45
Si	0.99	0.99		1.98	1.98	1.99	1.98	3.57	3.77	1.90		2.94	2.90
Ti	-	-		0.01	0.01	-	-	-	-	-		-	-
Al	-	-		0.02	0.02	-	-	0.27	0.41	0.11		1.09	1.06
Cr	-	-		0.02	0.02	-	-	0.02	0.02	0.02		-	-
Fe^{2+}	0.48	0.48		0.16	0.17	0.42	0.43	0.93	0.72	0.33		0.03	0.06
Ni	-	-		-	-	-	-	-	-	-		-	-
Mn	0.01	0.01		-	-	0.02	0.01	0.02	0.03	0.01		-	-
Mg	1.52	1.52		0.91	0.91	1.54	1.54	3.22	2.84	1.59		-	0.02
Ca	-	-		0.85	0.84	0.03	0.03	0.16	0.19	0.07		0.09	0.11
Na	-	-		0.04	0.04	-	-	0.07	0.07	0.02		0.69	0.81
K	-	-		-	-	-	-	-	-	-		0.06	0.04
Total	3.00	3.00		3.99	3.99	4.00	3.99	8.26	8.05	4.05		4.89	5.00
Oxygen	4	4		6	6	6	6	12	12	6		8	8
Fo	75.2	75.3	*En*	47.3	47.5	77.6	77.2	74.7	75.7	79.6	*Ab*	83.0	84.6
Fa	24.8	24.7	*Fs*	8.1	8.6	21.0	21.5	21.5	19.2	16.6	*An*	10.3	11.8
			Wo	44.6	43.9	1.4	1.2	3.8	5.1	3.8	*Or*	6.8	3.6
P, GPa									21.3	21.9			

Note: Numbers in parentheses are one standard deviations of the last significant digits. n, number of analyses; h-rock, host-rock; fragm, host-rock fragments in the SMVs; P, GPa - pressure estimation using the majorite barometer of Collerson et.al. (2010); b.d., below detection limit. The detection limit for each element is 0.3 wt.% (Lavrent'ev et al. 2015); n.d., not determined. Abbreviations: Ab, albite; En, enstatite; Fa, fayalite; Fo, forsterite; Fs, ferrosilite; Jd, plagioclase composition aggregate with jadeite; Melt – average chemical composition of interstitials between majorite-pyrope grains in the SMV matrix; Opx$_{Sem}$ – average chemical composition of low-Ca pyroxene from the SMVs in Pervomayskiy (Semenenko and Golovko, 1994); Maj-Prp, majorite-pyrope; Msk, maskelynite; Or, orthoclase; Wo, wollastonite.

TABLE 2. High-pressure mineral assemblages in different chondrites

Meteorite name	Type	High-pressure assemblage	SMV *PT* conditions		References
			P, GPa	T, °C	
Tenham	L6	Maj, Maj-Prp, Rwd, Akm, Prv, Mws	22–26	2000	Langenhorst et al. 1995; Tomioka and Fujino 1999
Sixiangkou	L6	Maj, Maj-Prp, Rwd, Akm, Mws, Lng, Jd_{sst}	20–24	2000	Chen et al. 1996; Zhang et al. 2006
Y-75100	H6	Maj-Prp + Opx +Ol, Wds, Rwd, Akm, Hol-Jd_{sst}	18–24	1900	Kimura et al. 2000 Tomioka and Kimura 2003; Miyahara et al. 2013
Suizhou	L6	Maj, Maj-Prp, Rwd, Hol, Tuite	18–22	1900	Xie et al. 2001, 2003
Y-75267	H6	Maj, Maj-Prp, Wds, Rwd, Akm, Hol	20	2000	Kimura et al. 2003
Y-791384	L6	Maj-Prp, Rwd, Akm, Hol, Jd_{sst}	18–23	2300	Ohtani et al. 2004; Miyahara et al. 2011, 2013
Y-74445	L6	Maj, Wds, Rwd, Akm, Hol, Jd_{sst}	17–24	2100	Ozawa et al. 2009
Taiban	L6	Maj+Cpx, Wds, Rwd, Lng, Jd_{sst}	17–20	1900	Acosta-Maeda et al. 2013
Pervomaisky	L6	Maj-Prp+Ol+Cpx, Jd_{melt}	13.5–15.0	1750–2150	This work
Sahara 98222	L6	Wds, Jd_{sst}	13–16	1900	Ozawa et al. 2009
Chelyabinsk	LL5	Jd_{melt}	3–12	<1700–2000	Ozawa et al., 2014
Novosibirsk	H5-6	Jd_{melt}	3–15	1400–2150	Bazhan et al., 2017

Note: PT-conditions in the SMV were estimated in previous studies. Abbreviations: Akm, akimotoite; Cpx, clinopyroxene; Hol, hollandite; Jd_{melt}, jadeite formed from the melt; Jd_{sst}, jadeite formed at the solid-state transformation of albitic feldspar; Lng, lingunite; Maj, majorite formed at the solid-state transformation of pyroxene; Maj-Prp, majorite-pyrope formed from the melt; Mws, magnesiowüstite; Ol, olivine; Opx, orthopyroxene; Prv, Mg-perovskite (bridgmanite), Rwd, ringwoodite; Wds, wadsleyite.

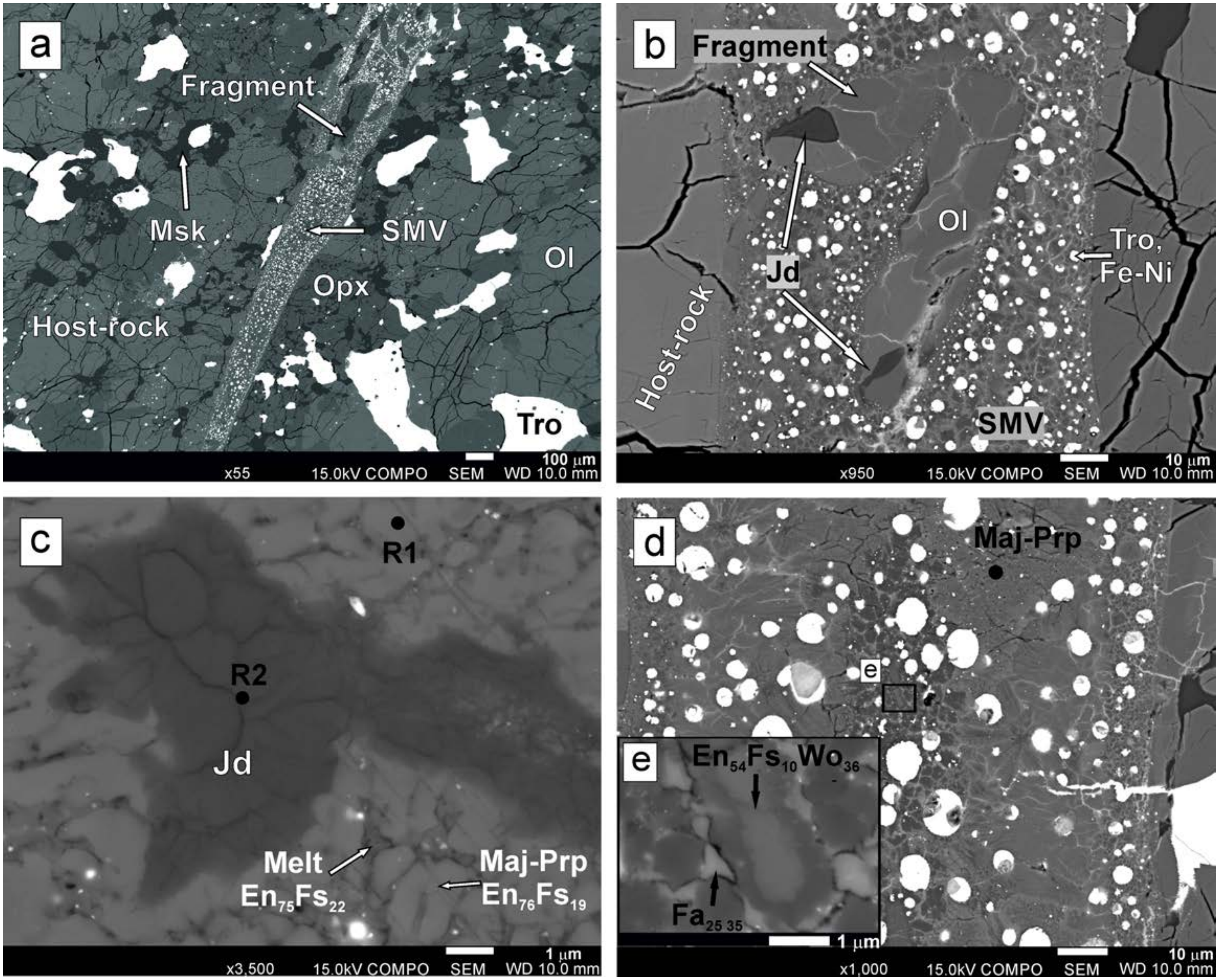
a
Fragment
Msk
SMV
Ol
Opx
Host-rock
Tro
x55 15.0kV COMPO SEM 100 μm WD 10.0 mm
b
Fragment
Ol
Tro, Fe-Ni
Jd
Host-rock
SMV
x950 15.0kV COMPO SEM 10 μm WD 10.0 mm
c
R1
R2
Jd
Melt $En_{75}Fs_{22}$
Maj-Prp $En_{76}Fs_{19}$
x3,500 15.0kV COMPO SEM 1 μm WD 10.0 mm
d
Maj-Prp
e
e
$En_{54}Fs_{10}Wo_{36}$
$Fa_{25\ 35}$
1 μm
x1,000 15.0kV COMPO SEM 10 μm WD 10.0 mm

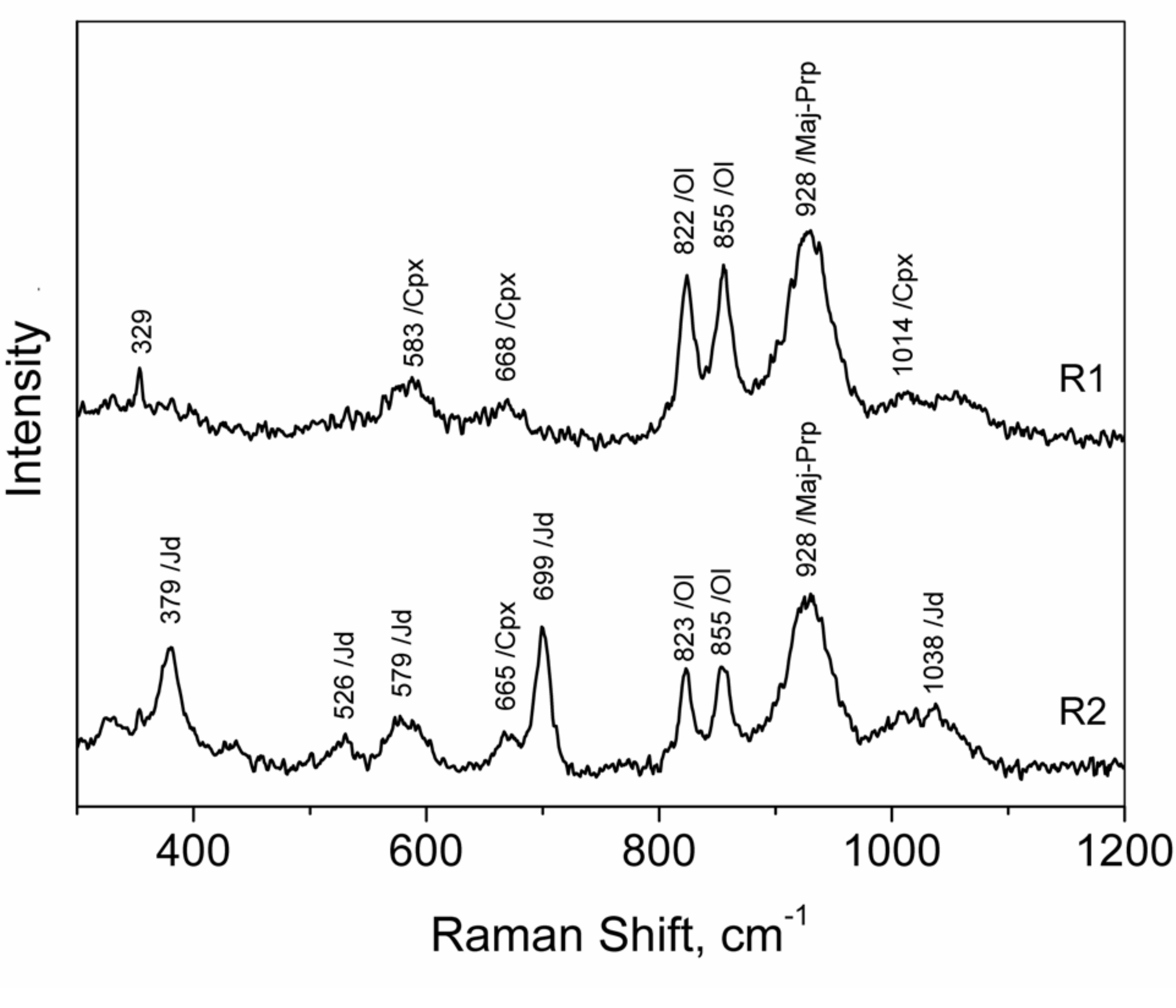
Intensity
329
583 /Cpx
668 /Cpx
822 /Ol
855 /Ol
928 /Maj-Prp
1014 /Cpx
R1
379 /Jd
526 /Jd
579 /Jd
665 /Cpx
699 /Jd
823 /Ol
855 /Ol
928 /Maj-Prp
1038 /Jd
R2
400
600
800
1000
1200
Raman Shift, cm^{-1}

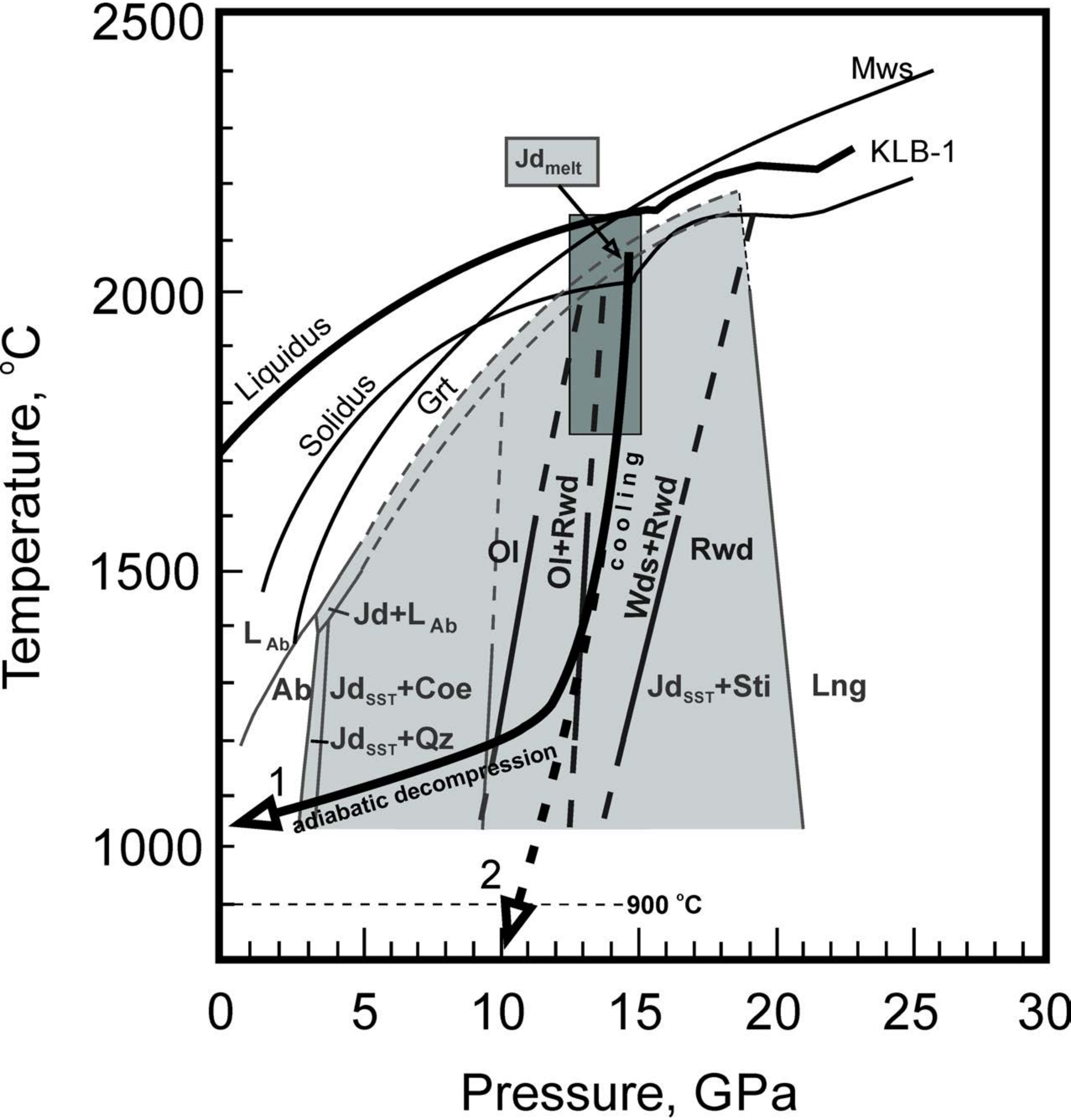
2500
2000
1500
1000
Temperature, °C
0
5
10
15
20
25
30
Pressure, GPa
Mws
KLB-1
Jd$_{melt}$
Liquidus
Solidus
Grt
cooling
Ol
Ol+Rwd
Wds+Rwd
Rwd
L$_{Ab}$
Jd+L$_{Ab}$
Ab
Jd$_{SST}$+Coe
Jd$_{SST}$+Qz
Jd$_{SST}$+Sti
Lng
1
adiabatic decompression
2
900 °C

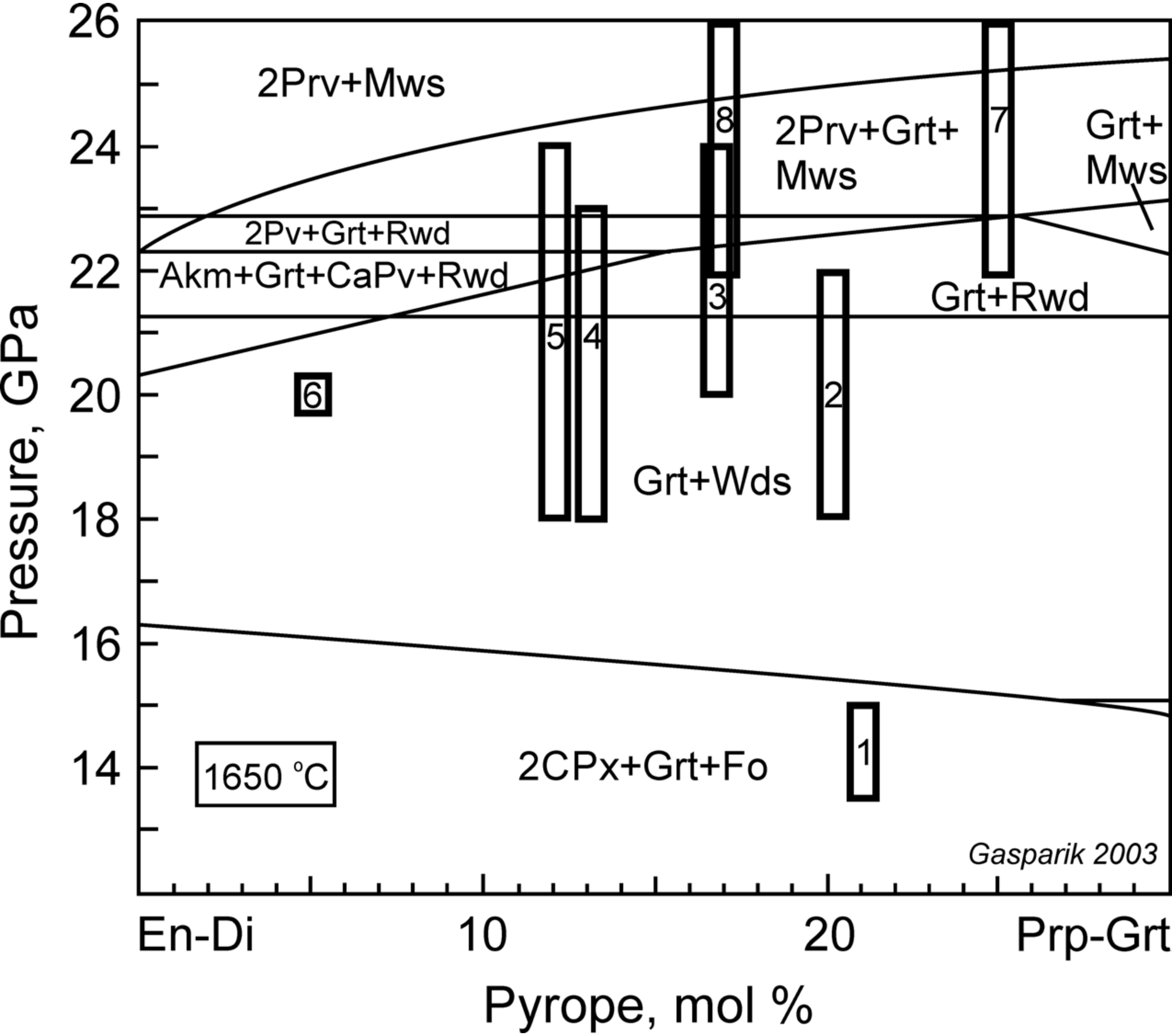
2Prv+Mws
8
2Prv+Grt+
Mws
7
Grt+
Mws
2Pv+Grt+Rwd
Akm+Grt+CaPv+Rwd
3
Grt+Rwd
5
4
6
2
Grt+Wds
1
1650 °C
2CPx+Grt+Fo
Gasparik 2003
26
24
22
20
18
16
14
Pressure, GPa
En-Di
10
20
Prp-Grt
Pyrope, mol %